Clinical Imaging 71 (2021) 83–100

Contents lists available at ScienceDirect

Clinical Imaging

journal homepage: www.elsevier.com/locate/clinimag

Breast Imaging

Fibroadenomas: a multidisciplinary review of the variants

Isil Basara Akin *, Pinar Balci

Dokuz Eylul University School of Medicine Department of Radiology, Izmir, Turkey

ARTICLE INFO

Keywords:
Fibroadenoma
Magnetic resonance imaging
Mammography
Ultrasonography
Variants

ABSTRACT

Fibroadenomas are the most common benign breast lesions in women. Hormonal activities, particularly an increase in oestrogenic activity, have an important role in the aetiology of fibroadenomas. They are commonly detected incidentally. Most fibroadenomas have similar imaging findings and these lesions can be defined as simple fibroadenomas (SFAs). However, due to different histopathologic characteristics and components, variants of fibroadenomas have been described. These variants include; juvenile, giant, complex, myxoid, cellular, and hyalinised fibroadenomas. The diagnoses of these variants are important. They have different clinical behaviours, potential for malignant transformation, and treatment strategies. We present imaging findings of SFAs and other variants of fibroadenomas. To our knowledge, there is no review in which imaging findings of all fibroadenoma variants are presented together.

1. Introduction

Breast masses can be classified in a wide spectrum of aetiologies with malignant and benign diagnoses. Invasive ductal carcinoma is the most common malignant lesion whereas fibroadenoma is the most common solid benign breast lesion [1], with a reported prevalence of 15–23% in autopsied cases [2]. These lesions are more common in black women than in white women [2]. Although the incidence peaks during the third decade of life [2], 50–60% of benign breast lesions in adolescents and young female patients are fibroadenomas [3].

Hormonal activities, particularly an increase in oestrogenic activity, have an important role in the aetiology of fibroadenomas. As hormone-dependent neoplasms, the dimensions of fibroadenomas increase during pregnancy and lactation and then decrease during the perimenopausal period [4]. Oral contraceptive use before the age of 20 years increases the risk of fibroadenoma development [4,5]. An immunosuppressed status, Epstein–Barr virus infection, and organ transplantation using cyclosporine are additional risk factors for fibroadenoma development [6,7].

Fibroadenomas are often detected incidentally in the clinic as painless, palpable, and mobile masses. Approximately 10–20% of fibroadenomas are present as multiple or bilateral masses [8]. Their size varies, typically ranging from 2 to 3 cm [9]. The clinical behaviour also varies, exhibiting progression, a stable course, or regression during follow-up [9]. With rapidly progressing lesions, spontaneous infarcts, necrosis, or calcifications can develop [1].

Fibroadenomas arise from terminal duct lobular units [1]. Fibroadenomas present macroscopically as well-circumscribed, lobulated, and tan- or white-coloured, solid lesions with a rubber-like consistency. They may include calcifications and slit-like spaces [10]. Microscopic histopathologic evaluation shows biphasic lesions, consisting of stromal and epithelial components, with an epithelial proliferation surrounded by fibroblastic stroma [11].

The above macroscopic and microscopic histopathologic features describe classic fibroadenomas, which are defined as simple fibroadenomas (SFAs). However, due to different histopathologic characteristics and components, variants of fibroadenomas have been described, including juvenile, giant, complex, myxoid, cellular, and hyalinised fibroadenomas [12]. Recognition and diagnosis of these variants is critically important because they have different clinical behaviours, potential for malignant transformation, and treatment strategies. In this pictorial review, we aimed to present imaging findings of SFAs and other variants of fibroadenomas.

2. Fibroadenoma variants and typical imaging findings

2.1. Simple fibroadenoma

The microscopic histopathologic characteristics of SFAs have classic features; because there is no stromal atypia, the stromal cellularity is similar to that of perilobular stroma. Also, there is no or sparse mitotic activity [7].

* Corresponding author.
E-mail addresses: slbasara@yahoo.com (I. Basara Akin), pinar.balci@deu.edu.tr (P. Balci).

https://doi.org/10.1016/j.clinimag.2020.10.058
Received 11 June 2020; Received in revised form 2 October 2020; Accepted 26 October 2020
Available online 6 November 2020
0899-7071/© 2020 Elsevier Inc. All rights reserved.

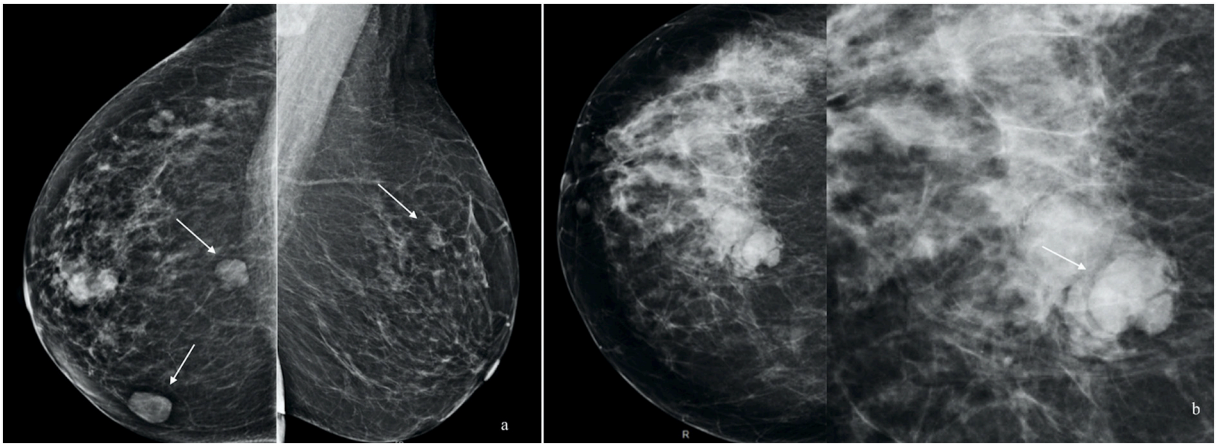


Fig. 1. MG images of two different patients; round and oval shaped, isohyperdense, well circumscribed SFAs are seen (arrows) (a). Perilesional thin halo sign due to the Mach effect is seen (arrows) (b).

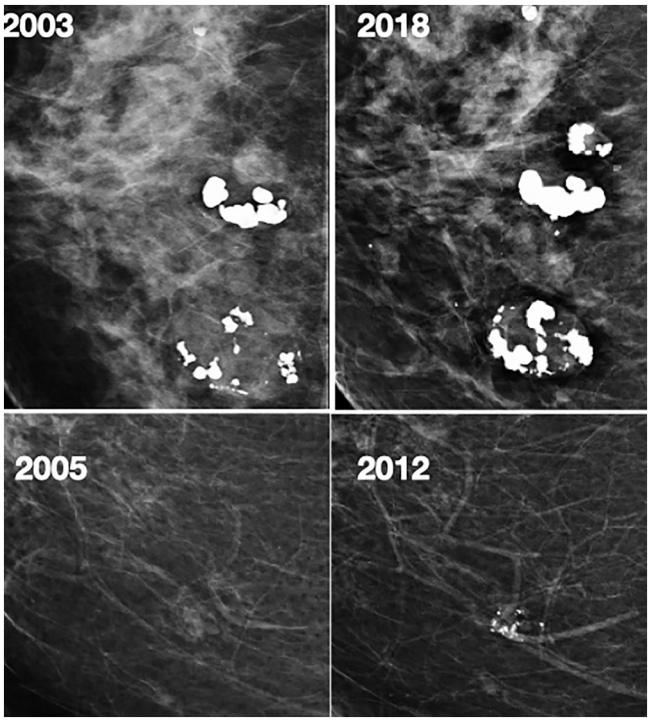


Fig. 2. MG images of three different patients; involutional, benign calcifications are detected. In a 53-year-old female patient, the occurrence and proliferation of benign popcorn calcifications from peripheral to central zone between 2003 and 2018 are seen (a). In a 57-year-old female patient, there are dystrophic calcifications occurred at early stage of involution (arrow) (b).

On mammography (MG) examination, the lesion shape is typically round or oval and may have macrolobulated features, the contours are well circumscribed, and the lesion may be isodense or hyperdense. Perilesional thin halo sign is frequently seen due to the Mach effect (Fig. 1). At postmenopausal period over the fifth and sixth decades, SFAs may exhibit involutional changes and thus calcifications that are benign and coarse. Calcifications first occur in the peripheral part of the lesion, and over time these calcifications conjoin and become rough, called popcorn calcifications (Fig. 2). The importance of this finding is that no further routine follow-up procedure is needed for these lesions. However, dystrophic calcifications can occur early on with these involutional calcifications, and it is often difficult to distinguish them from suspicious malignant calcifications, such as pleomorphic ones (Fig. 2). For these lesions, biopsy and possible excisional procedures are needed to determine the exact diagnosis [1,9].

Nevertheless, MG findings commonly overlap with the imaging findings of other benign lesions, such as cysts, or those of well-defined malignant lesions. As a result, an additional imaging method, typically ultrasonography (US), is used. US examination shows the internal characteristics of the lesions. In US examination, the shape and contour features of the lesions are similar to those on MG. Echotexture is homogeneous and either isoechoic or hypoechoic. One important characteristic of US findings of especially SFAs is the orientation of the lesion, which is parallel to breast tissue and skin. Another important finding of SFAs is internal echogenic fibrous septa [13]. As a result of peripheral breast parenchymal compression by the lesion, a pseudocapsule may form, which is seen as an echogenic perilesional structure [14]. When involutional changes such as necrosis or calcifications occur, the echotexture becomes heterogeneous [1,14]. Less acoustic enhancement than that of cysts, edge enhancement, and abrupt interfaces are commonly seen. However, if calcifications occur, acoustic shadowing may be seen (Fig. 3) [15]. Coloured Doppler US examination reveals vascularisation in 80% of SFA cases, and this is more common in young patients (Fig. 4) [14,16].

On US elastography, most SFAs have low stiffness, with similar findings to those of the adjacent breast tissue. On strain elastography, the lesions typically have an elasticity score of 1–3. Calcifications resulting from involutional changes or fibroadenomas >2 cm may result in a false-positive malignancy with high stiffness, with a score of 4 or 5 [17]. Additionally, due to peri- and intralesional compression and capsule stretch, elastographic findings sometimes show malignant lesion features (Fig. 4) [18,19].

The magnetic resonance imaging (MRI) findings of SFAs also vary.

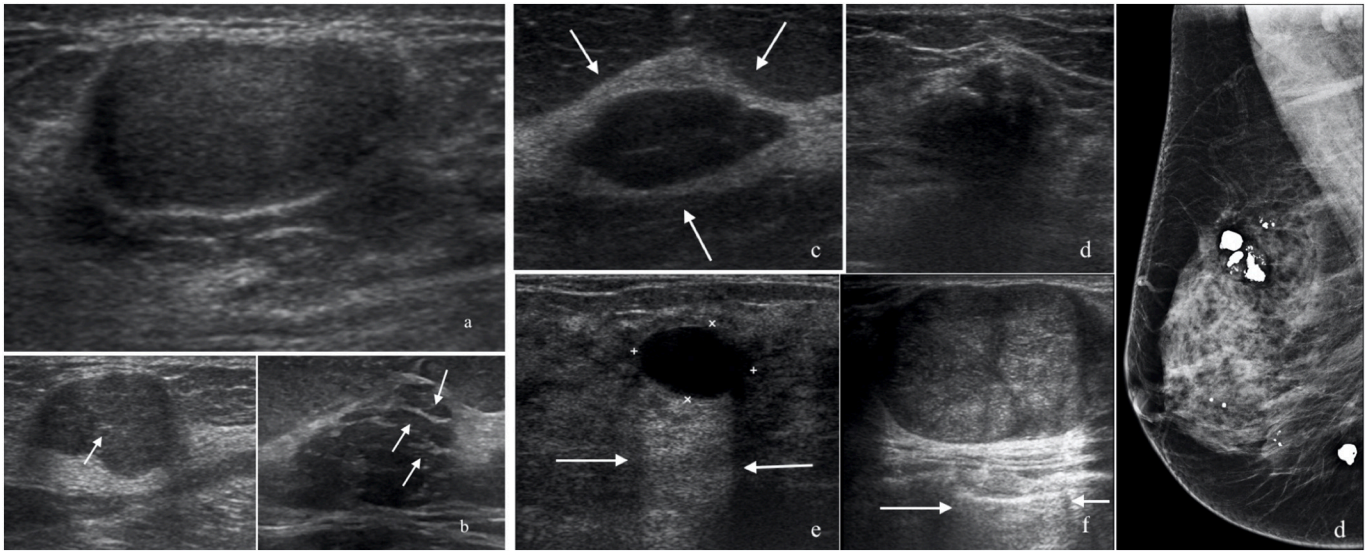


Fig. 3. B mod US image of 32-year-old female patient; there is oval shaped, well circumscribed, hypoechoic solid lesion. The lesion is in parallel orientation to breast tissue and skin (a). US images of two different SFAs; there are echogenic fibrous septa (arrows) (b). A-36-year-old female patient, ovoid, well defined, SFA diagnosed lesion, US image reveals an echogenic perilesional pdeudocapsular structure formed due to peripheral breast parenchymal compression (arrows) (c). Heterogeneous, irregular shaped, vertical orientated solid lesion. There is a posterior acoustic shadowing. In MG examination there are calcifications in this SFA diagnosed lesion (d). US images of a cyst (e) and SFA (f); there are posterior acoustic enhancements (arrows). The enhancement is cleaner in cyst.

Shape and contour features are similar to those seen on MG and US. On T1-weighted images, the lesion is isointense with the surrounding breast tissue. T2 signals change according to the content of the lesion. Typically, in dynamic sequences, progressive enhancement is seen. An important MRI finding is non-enhancing hypointense internal septa in an enhancing solid lesion; in more than 95% of SFA, this finding is diagnostic. However, the absence of internal septa does not rule out an SFA (Fig. 5) [20].

2.2. Juvenile fibroadenoma

Juvenile fibroadenoma (JFA) is a rare (7–8%) fibroadenoma variant [1,21]. JFAs are commonly seen in adolescents between the ages of 10 and 18 years [21]. On macroscopic histopathologic evaluation, the lesions are typically circumscribed. Microscopic histopathology reveals both stromal and epithelial hypercellularity [22]. Clinically, JFAs are painless and enlarge rapidly; this rapid growth can cause aesthetic problems as a result of breast hypertrophy or asymmetry [23], and ulceration in the skin and superficial venous distension may be seen [1]. JFAs are common in African American adolescents and frequently present as multiple, bilateral lesions in this population [22].

As JFAs are commonly seen during early childhood and adolescence, on radiologic evaluation, MG examination is neither recommended nor necessary [24]; US is the main diagnostic examination. The US features of JFAs are similar to those of SFAs, with a circumscribed oval shape, parallel orientation, hypo-isoechoic echotexture, and posterior acoustic enhancement may also be seen [25,26]. Increased vascularity is typically seen on Doppler US [26]. The sonoelastographic and MRI findings of JFAs are similar to those SFAs (Fig. 6). T1 signals are hypo-isointense, whereas T2-weighted images are typically hyperintense as a result of hypercellularity. Enhancement changes the characteristics, and, like SFA, non-enhanced internal hypointense septa are seen. The clinical findings, patient's age, and lesion size >5 cm are important characteristics for JFA diagnosis [27].

2.3. Giant fibroadenoma

Giant fibroadenoma (GFA) is another rare (0.5–2%) variant of fibroadenomas. GFAs are large (>5 cm, >500 g) lesions [27,28] seen in women during the premenopausal period, particularly before the age of 30 years [29]. In fact, GFAs in patients between the ages of 10 and 18 years are defined as JFAs, which eventually become GFAs as a result of rapid growth [30]. GFAs are most common in African American as well as East Asian females. Similar to JFAs, rapid growth can cause aesthetic problems as a result of breast hypertrophy and asymmetry [23]. All imaging features are similar to those of JFAs (Fig. 7).

2.4. Complex fibroadenoma

An important variant of fibroadenoma is complex fibroadenoma (CFA), defined as fibroadenoma comprising at least one or more complex pathologic characteristics, including cysts >3 mm, epithelial calcifications, sclerosing adenosis, and papillary apocrine metaplasia [31]. CFAs comprise 22% of histopathologically proven fibroadenomas. The presence of a CFA increases the risk of invasive breast cancer development 3.1 fold compared with the normal population; the risk of invasive breast cancer is increased 1.89 fold in women with SFAs. Both in the normal population and women with SFAs or CFAs, an increased malignancy risk is typically related to perilesional benign proliferative changes and an elevated familial risk of breast cancer [32]. Additionally,

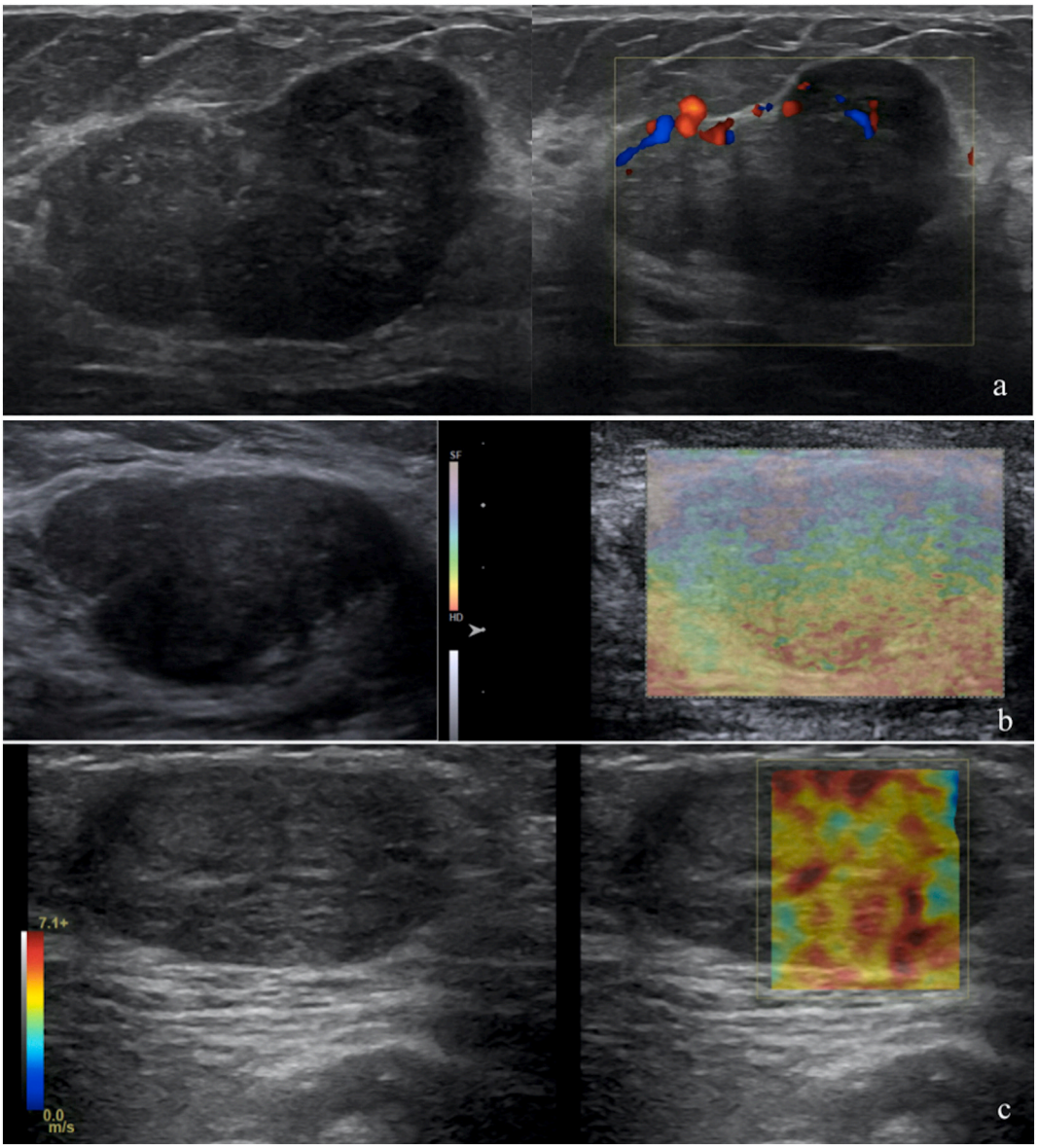


Fig. 4. Doppler US image of a 25-year-old female patient shows peripheral vascularization (a). Strain elastography images of a 42-year-old female patient, the lesion has low stiffness and in colour map, blue-green colours are dominant (b). A SFA diagnosed and 5 cm measured solid lesion includes focal areas with high stiffness (c). (For interpretation of the references to colour in this figure legend, the reader is referred to the web version of this article.)

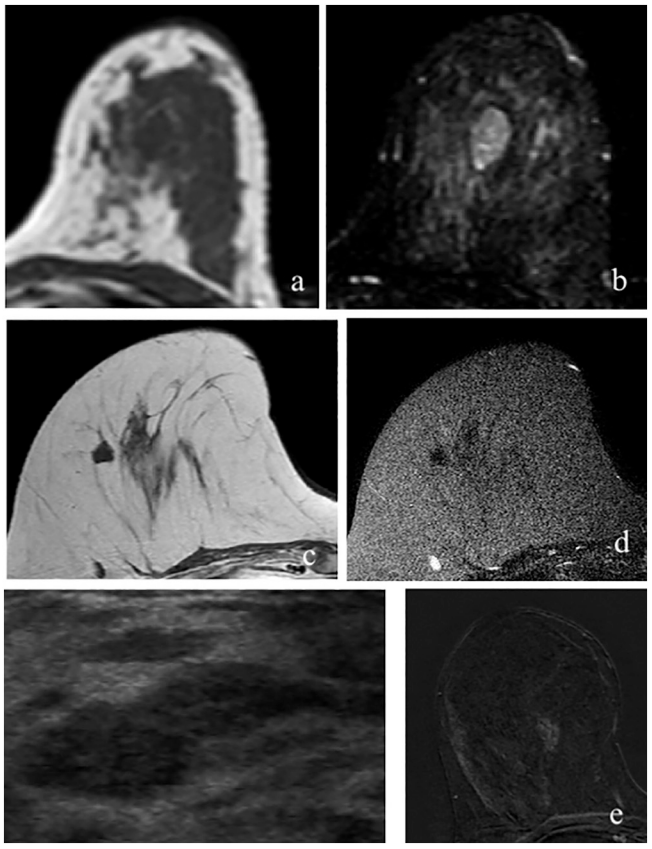


Fig. 5. MRI images, in a 51-year-old female patient, the lesion is hypointentense on T1 weighted (a), hyperintense on T2 weighted (b) images. In other 47-year-old female patient, the lesion is hypointense in both T1 and T2 weighted (c–d) images. US and subtraction MRI images of SFA diagnosed lesion reveal hyperechogen and hypointense, non-enhancing internal septa (arrows) (e).

this increased malignancy risk is not limited to the lesion site; any site in the same or contralateral breast may be affected by the malignancy [32]. Patients who have changes in their lesions which are followed-up or patients with imaging BI-RADS 4 findings biopsy applications are applied. Treatment approaches may vary in CFAs. In our institution, although it may be a very protective approach, our protocol is total excision of complex fibroadenomas when diagnosed in core biopsy. As a result, the treatment of CFAs is total surgical excision with clean margins and close optimal radiologic follow-up [33].

Although there is an increased risk of malignancy with CFAs, the imaging findings of CFAs are fundamentally similar to those of SFAs. On MG, CFAs are generally well defined with a round or oval shape. Lesions may include either popcorn or coarse heterogeneous calcifications. Focal asymmetry can be seen in a limited number of cases (Figs. 8,. 9) [34].

The US findings of CFAs resemble the MG findings, with no distinctive features [35]. Pinto et al. reported that most CFAs are oval, circumscribed, and parallel in orientation with no posterior acoustic enhancement or calcification content (Fig. 9) [36]. Despite this, an irregular shape, non-circumscribed contour, complex echo pattern, microcalcification content, and posterior acoustic enhancement are more common in CFAs than in other fibroadenoma variants [36]. Those authors concluded that the most relevant findings of CFAs are a heterogeneous echotexture, non-circumscribed margin with posterior acoustic enhancement, and parallel orientation. Additionally, they showed that epithelial calcification and cysts >3 mm are more common among CFAs (Fig. 10) [36].

To our knowledge, no study has specifically described the US elastographic findings of CFAs. As B-mode US findings, US elastography findings are similar to SFAs. In strain elastography, the elasticity score of CFAs is typically 1, 2, or 3. CFAs with a large size and calcification content are stiffer, which can cause false-positive results (Fig. 10).

The MRI findings of CFA are similar to those of SFAs and other fibroadenoma variants, with no specific, distinctive finding (Fig. 11).

2.5. *Myxoid fibroadenoma*

Myxoid fibroadenoma (MFA) is a histologic subtype of fibroadenomas with abundant myxoid matrix content and a hypocellular stroma [37]. MFAs may be associated with Carney complex [38], an autosomal dominant syndrome characterised by endocrine over-activity and spotty skin pigmentation; these MFAs have an increased risk of non-breast tumour development. The associated tumours are mainly myxomas (cardiac or cutaneous), pituitary adenomas, or psammomatous melanotic schwannomas [39].

On radiologic evaluation, MG and US findings do not show any distinctive characteristics (Figs. 12, 13). In most MFA cases, the MRI findings are similar to those of other variants, such as hypointense T1 and hyperintense T2 signals. In dynamic images, MFAs demonstrate prominent, rapid enhancement with washout. Pharmacokinetically, type 3 signal-intensity curves are seen, suggestive of malignancy (Fig. 14) [40].

2.6. *Cellular fibroadenoma*

Cellular fibroadenoma (CeFA) is a fibroadenoma variant characterised by high stromal cellularity that is uniform and lacks stromal atypia [41,42]; the cellularity can be classified as focal or mild. CeFAs are usually seen in young women, and the cellularity declines with age [43]. On histopathologic evaluation, there are overlapping features, particularly with benign phyllodes tumours (PT). Under core-needle biopsy, a diagnosis of CeFA can change to one of PT or vice versa after surgical examination (Fig. 15) [41].

There are no distinguishing radiologic characteristics of CeFAs (Fig. 16).

2.7. *Hyalinised fibroadenoma*

Hyalinised fibroadenoma (HFA) is another variant of fibroadenoma, particularly found in older women, with less cellular and more sclerotic patterns. Hyalinisation and necrotic changes accompany epithelial atrophic changes, and calcifications usually develop [44,45]. These calcifications are either popcorn, coarse, eggshell, or suspicious, such as

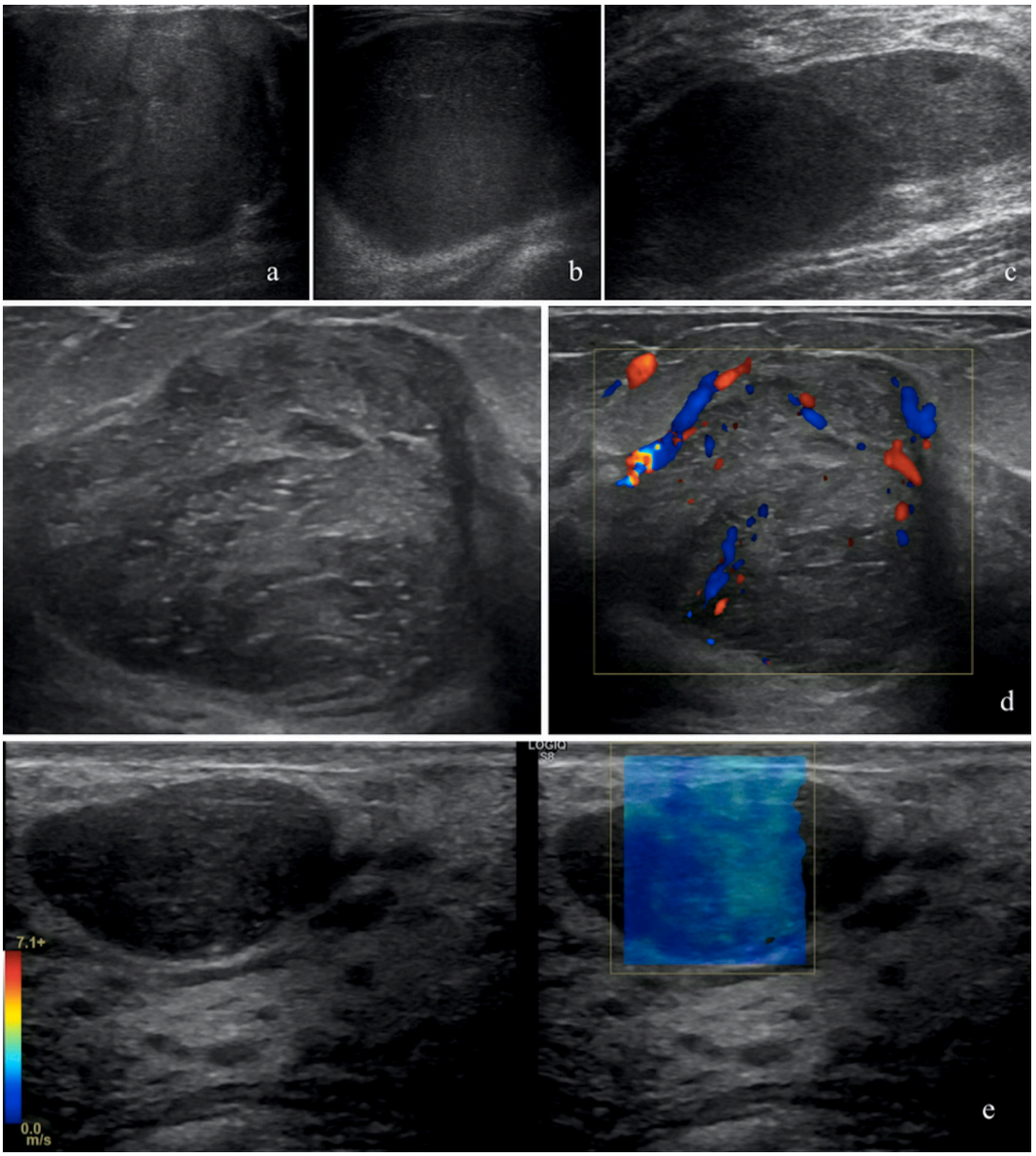


Fig. 6. B mod US images of different JFA diagnosed patients; a 14-year-old (a), a 16-year-old (b), and a 22-year-old (c) patients. The lesions are hypo-isoechoic and minimal heterogeneous with round (a, b) and oval (c) shapes. The lesions have circumscribed margins. Doppler US image reveals increased vascularity in the lesion, which is diagnosed as JFA (d). Strain elastography in JFA shows diffuse blue colour compatible with low stiffness (e). (For interpretation of the references to colour in this figure legend, the reader is referred to the web version of this article.)

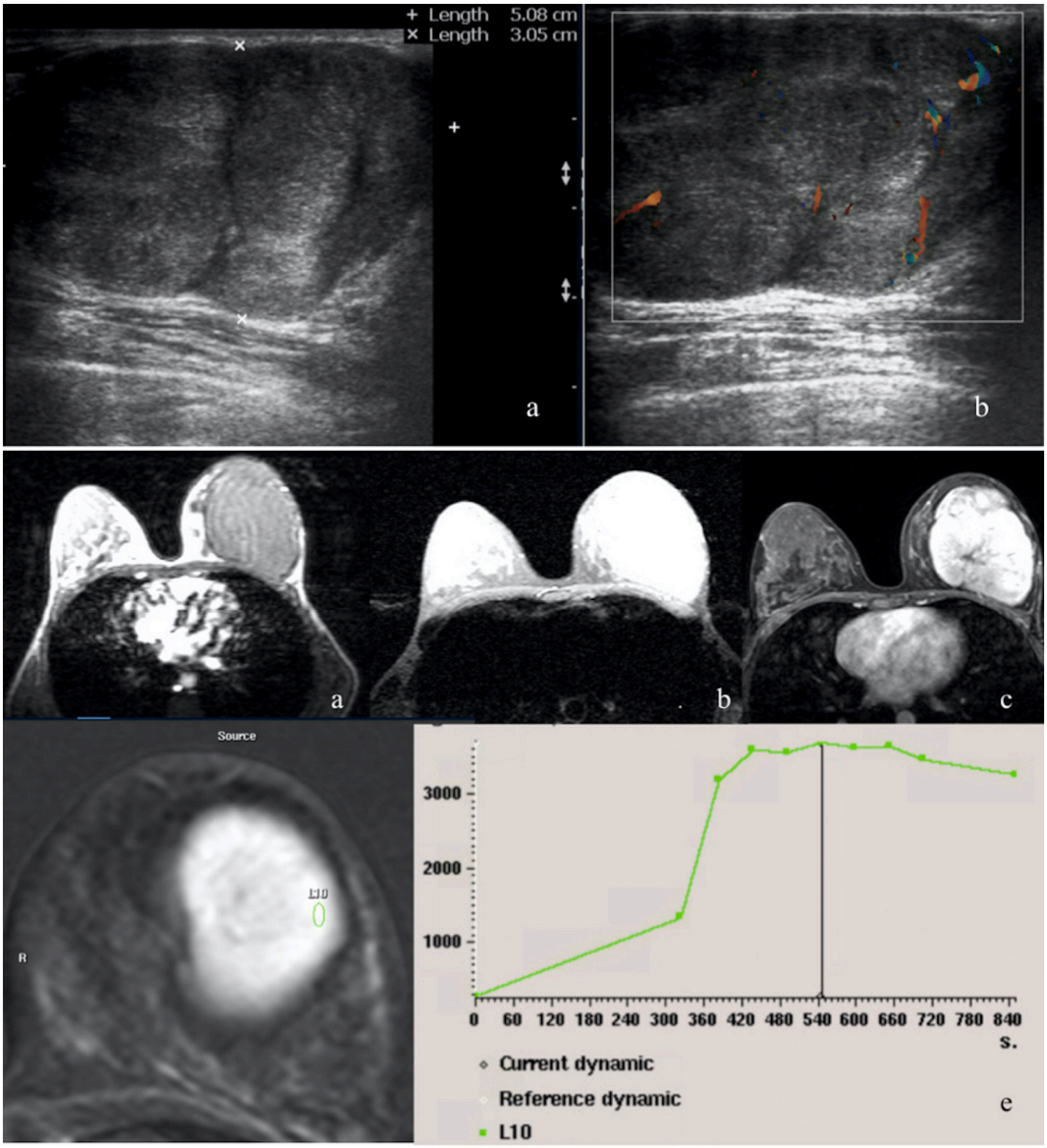


Fig. 7. B mod US (a) and Doppler US (b) images of a 23-year-old female patient with GFA; the lesion is in round shape with lobulated margins. Lesion is hypoechoic with minimal heterogeneous echotexture. Additionally, there is a prominent posterior acoustic enhancement. Minimal vascularity is seen in the lesion. MRI images of a16-year-old female patient with GFA; the giant lesion is hypointense on T1 weighted (c), hyperintense on T2 weighted (d) images. The lesion has avid and diffuse enhancement on dynamic sequence (e) and shows type 2 signal-intensity curve (f).

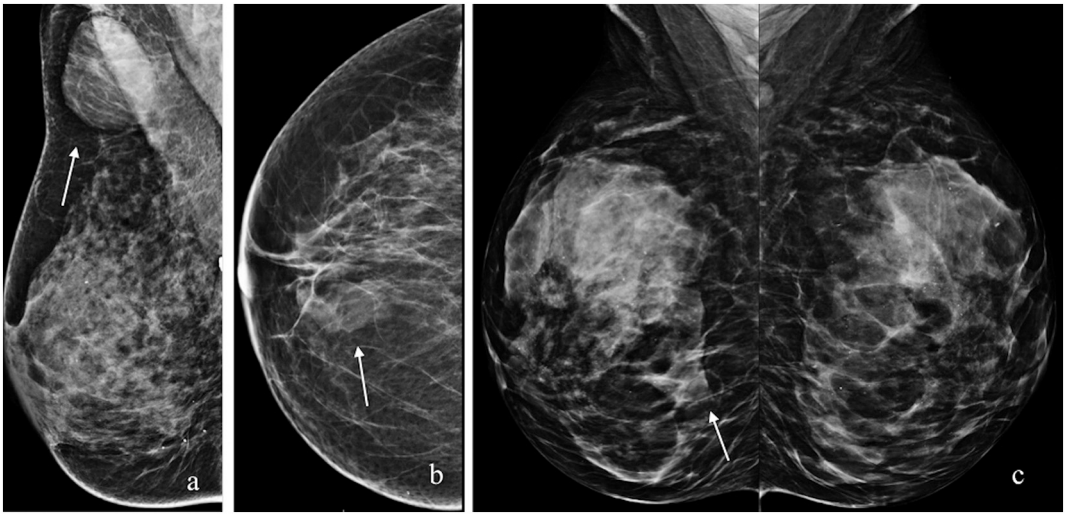


Fig. 8. MG images of different CFAs; the lesion is oval shaped, well defined and hyperdense (arrow) (a). Isodense lesion shows microlobulated and obscured margins (arrow) (b). There is an asymmetric increased density at the lower quadrant of right breast in the area of the lesion (arrow) (c).

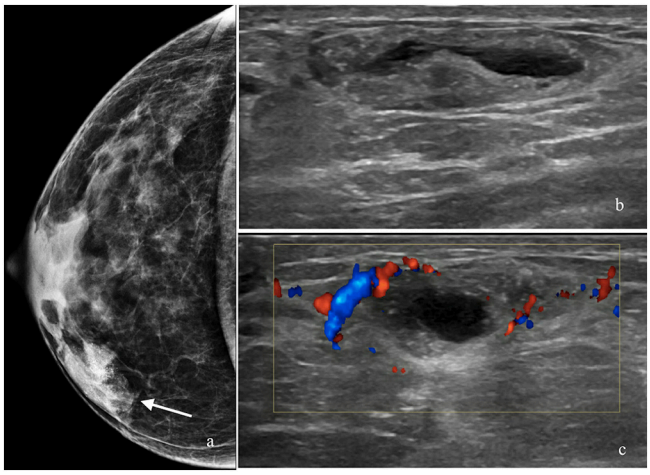


Fig. 9. MG (a), B mod US (b) and Doppler US (c) images of a 37-year-old female patient with CFA; in MG image, there is an oval, hyperdense nodular lesion at the inner quadrant of the right breast. The lesion includes multiple, clustered pleomorphic calcifications (arrow). US image shows parallel orientation, echogenic milimetric calcification, and no acoustic enhancement and there is cystic component in the lesion. In the solid components of the lesion Doppler US reveals increased vascularities.

pleomorphic, linear, or branching [45].

MG is an important imaging method especially for HFAs. As patients with HFAs are typically older than those with other fibroadenoma variants, MG is frequently used as the initial imaging method, with calcification being an important finding. Benign ones, such as popcorn or capsular calcifications, do not cause any problem for diagnosis or follow-up and are predominantly located at marginal peripheral sites of the lesion [45]. However, suspicious types, such as pleomorphic or branching calcifications, are challenging for diagnosis: these patients are commonly referred for biopsy. The size and distribution of the calcifications are important in the evaluation (Fig. 17). Microcalcifications with linear segmental distribution are thought as suspicious for malignancy [45]. As a result of hyalinisation and necrosis, degeneration, and involutions occur, and these changes result in suspicious imaging findings, such as an irregular shape and obscured, microlobulated, indistinct, and spiculated margins. HFAs have a variety of densities, but high-density lesions are predominant (Fig. 18) [44,45].

To our best knowledge, there are no studies that specifically described the US findings of HFAs. However, according to our experience, US typically shows heterogeneous lesions, resulting from degenerative changes, similar to the MG findings. The margin and shape features of HFAs are similar on MG and US. As a result of the calcification content, posterior acoustic shadowing is a common finding on US. Doppler US findings cannot differentiate HFAs from other variants. On sonoelastography, the lesion becomes stiffer as the calcification content increases (Fig. 19).

On MRI, HFAs have different T1 and T2 signals. In a dynamic sequence, HFAs show low and slow enhancement because of sclerotic and hyalinised changes (Fig. 20) [46].

Distinctive imaging and special findings of different variants are shown in the table (Table 1).

3. Radiologic evaluation and follow-up

Fibroadenomas may be classified as BI-RADS 3 lesions according to their imaging findings. Round or oval shape, circumscribed margins, parallel orientation, internal hyperechogenic septa, no or low posterior acoustic enhancement, and low enhancement with non-enhancing internal hypointense septa are typical findings of fibroadenoma, which are compatible with the BI-RADS 3 classification [46–48]. Fibroadenomas with course or popcorn calcifications may be classified as BI-RADS 2.

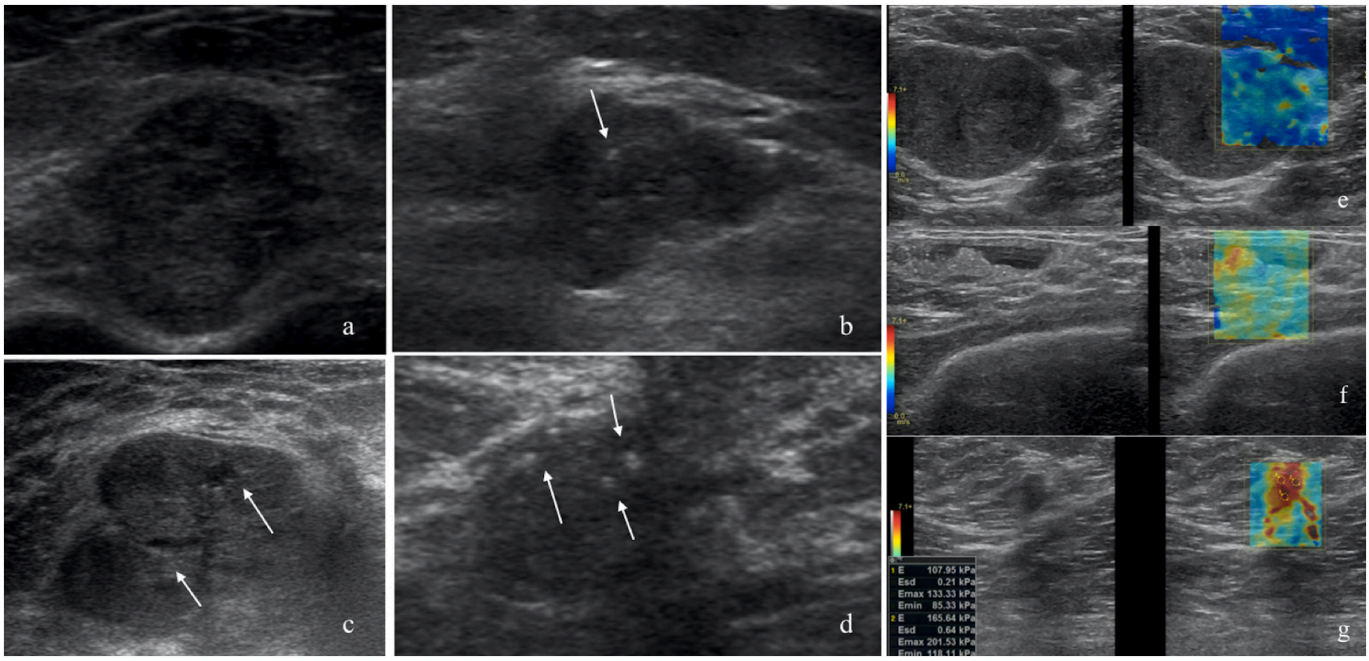


Fig. 10. B mod US images of CFA diagnosed patients. The lesions have heterogeneous echotextures. Lesions are oval-round (a, b and c) and irregular (d) shapes. All the lesions have non-circumscribed margins and all of them are in vertical orientations. Lesions include epithelial calcifications (arrows) (b, d) and cysts (arrows) (c). Strain (e, f) and shear-wave (g) elastography images; the lesions have different stiffness. Shear-wave elastography reveals high stiffness values. This lesion is diagnosed as CFA with chondroid metaplasia. The authors thought that the high values had been dependent on these metaplastic changes.

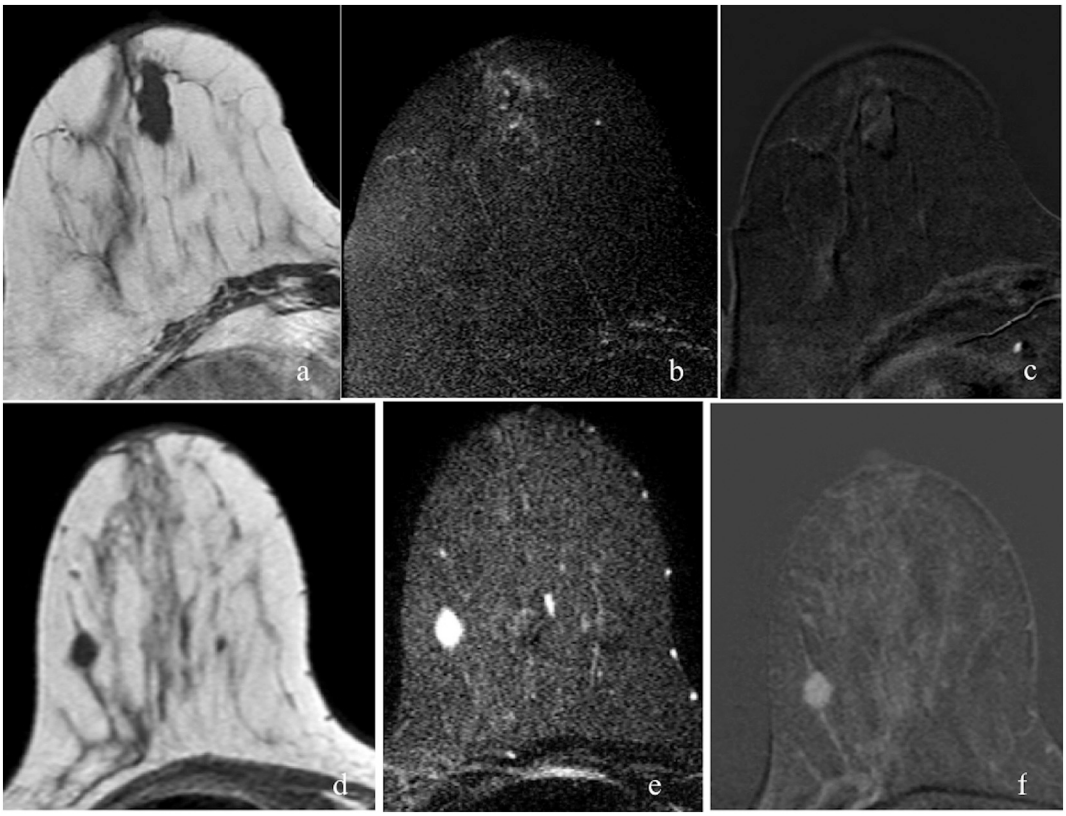


Fig. 11. MRI images, in 42-year-old female patient (a, b and c) and 35-year-old patient (d, e and f) with CFAs; the lesions are both hypointentense on T1 weighted images (a, e), hypointense with milimetric focal hyperintensities (b) and hyperintense (e) on T2 weighted images. In dynamic sequences, the lesion in the first patient shows very low enhancement (c) whereas the other lesion shows prominent enhancement (f).

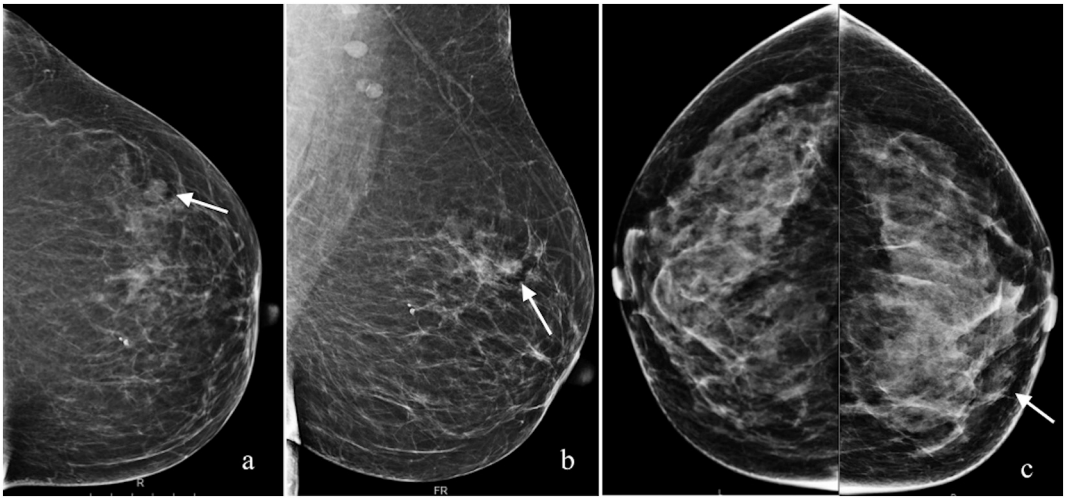


Fig. 12. MG images of three different patients with MFAs; the lesion is oval shaped, well defined and isodense (arrow) at the outer quadrant of left breast (a). Hyperdense, non-circumscribed lesion shows obscured margins (arrow) (b). There is an asymmetric increased density at the lower quadrant of left breast in the area of the lesion (arrow) (c).

Additionally, fibroadenomas that remain stable after 24 months are downgraded to BI-RADS 2.

In some cases, the imaging findings are challenging. Lesions with suspicious findings are classified as BI-RADS 4A according to the MG, US and MRI findings as BI-RADS 4. BI-RADS 4 lesions have a rate of malignant transformation of 3–10% for BI-RADS 4A, 10–50% for BI-RADS 4B and 50–95% for BI-RADS 4C [48]. When they include suspicious imaging features all fibroadenoma variants may be classified as BI-RADS 4A/4B/4C, but this particularly true for CFAs and CeFAs with suspicious imaging findings. Irregular shapes, non-circumscribed margins, non-parallel orientations, heterogeneous echogenicities, and posterior acoustic shadowing are suspicious imaging findings compatible with BI-

Table 1
Distinctive imaging and special findings of different variants

Fibroadenoma variant	Mammography	Ultrasonography	Magnetic resonance imaging	Specific findings
Simple fibroadenoma	Do not show any distinctive characteristics	Do not show any distinctive characteristics	Non-enhancing hypointense internal septa in an enhancing solid lesion; in more than 95% of SFA	The microscopic histopathologic characteristics have classic features; because there is no stromal atypia, the stromal cellularity. There is no or sparse mitotic activity
Juvenile fibroadenoma	Neither recommended nor necessary	Increased vascularity is typically seen on Doppler US	T2-weighted images are typically hyperintense as a result of hypercellularity	Commonly seen in adolescents between the ages of 10 and 18 years. They are painless and enlarge rapidly
Giant fibroadenoma	All imaging features are similar to those of JFAs	All imaging features are similar to those of JFAs	All imaging features are similar to those of JFAs	They are seen in women during the premenopausal period, particularly before the age of 30 years. Patients between the ages of 10 and 18 years are defined as JFAs, which eventually become GFAs as a result of rapid growth
Complex fibroadenoma	Do not show any distinctive characteristics	Most relevant findings are heterogeneous echotexture, non-circumscribed margin with posterior acoustic enhancement, and parallel orientation. Additionally, epithelial calcification and cysts >3 mm are more common	Do not show any distinctive characteristics	The presence of a CFA with perilesional benign proliferative changes and an elevated familial risk of breast cancer may increase the risk of invasive breast cancer development
Myxoid fibroadenoma	Do not show any distinctive characteristics	Do not show any distinctive characteristics	High signal intensity on T2 weighted images Rapid wash-out on dynamic images	May be associated with Carney complex
Cellular fibroadenoma	Do not show any distinctive characteristics	Do not show any distinctive characteristics	Do not show any distinctive characteristics	Overlapping histopathologic features, particularly with benign phyllodes tumours. Diagnosis of CeFA can change after surgery
Hyalinised fibroadenoma	MG is frequently used as the initial imaging method, with calcification being an important finding	Lesions may be heterogeneous, resulting from degenerative changes, similar to the MG findings	They show low and slow enhancement because of sclerotic and hyalinised changes	Particularly in older women, with less cellular and more sclerotic patterns

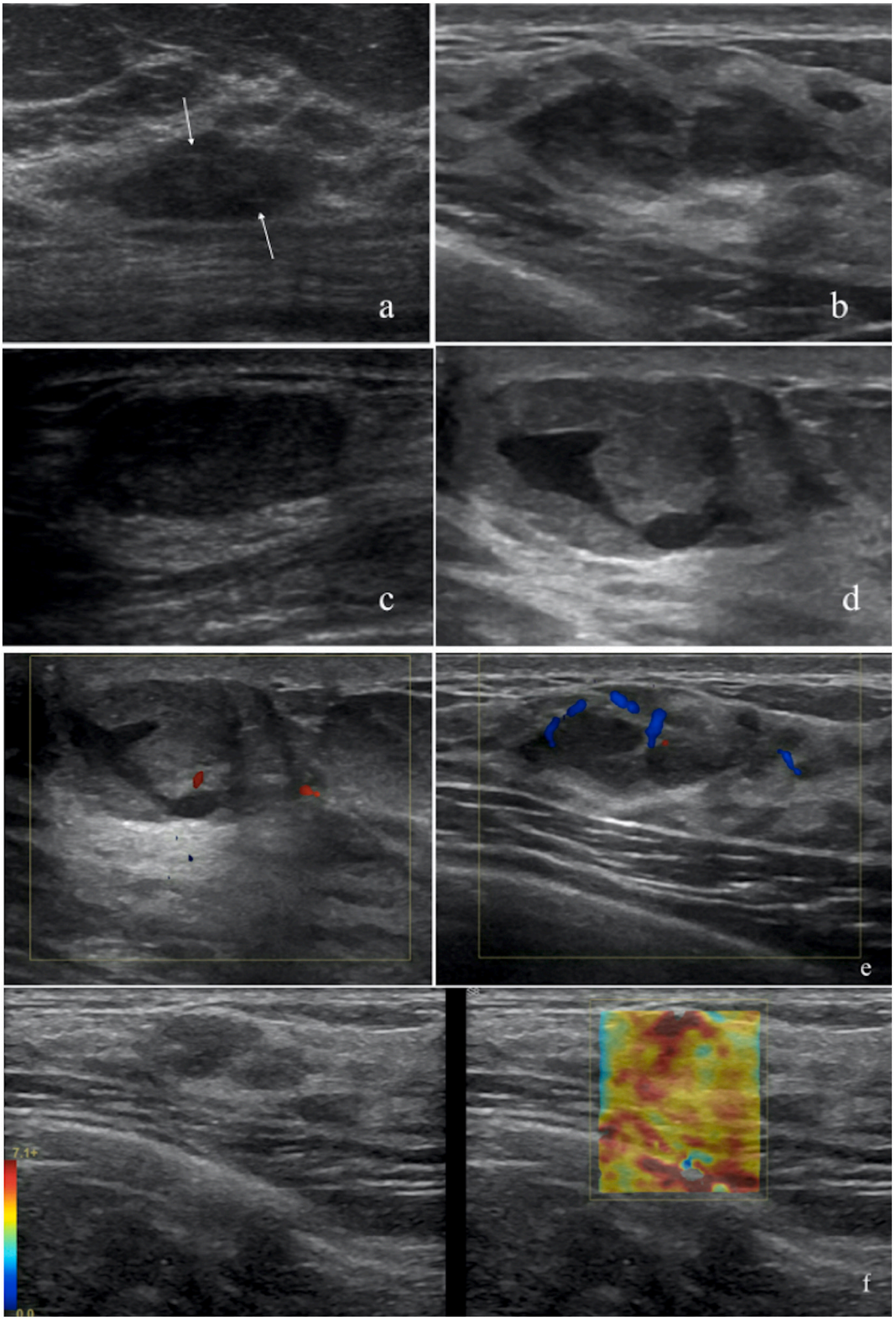


Fig. 13. B mod US images MFAs in four different patients. The lesion is in parallel orientation, oval shaped, hypoechoic, with internal echogenic septa (arrows) (a). There is bilobulated, hypoechoic, oval shaped solid lesion with posterior acoustic enhancement (b). The lesion has well defined contour and oval shape. There is posterior acoustic enhancement (c). The complex cystic lesion is isoechoic and there is posterior acoustic enhancement (d). Doppler US images of two different MFAs show mild vascularization in the lesions (e, f). Strain elastography examination reveals stiffer areas in the lesion (g).

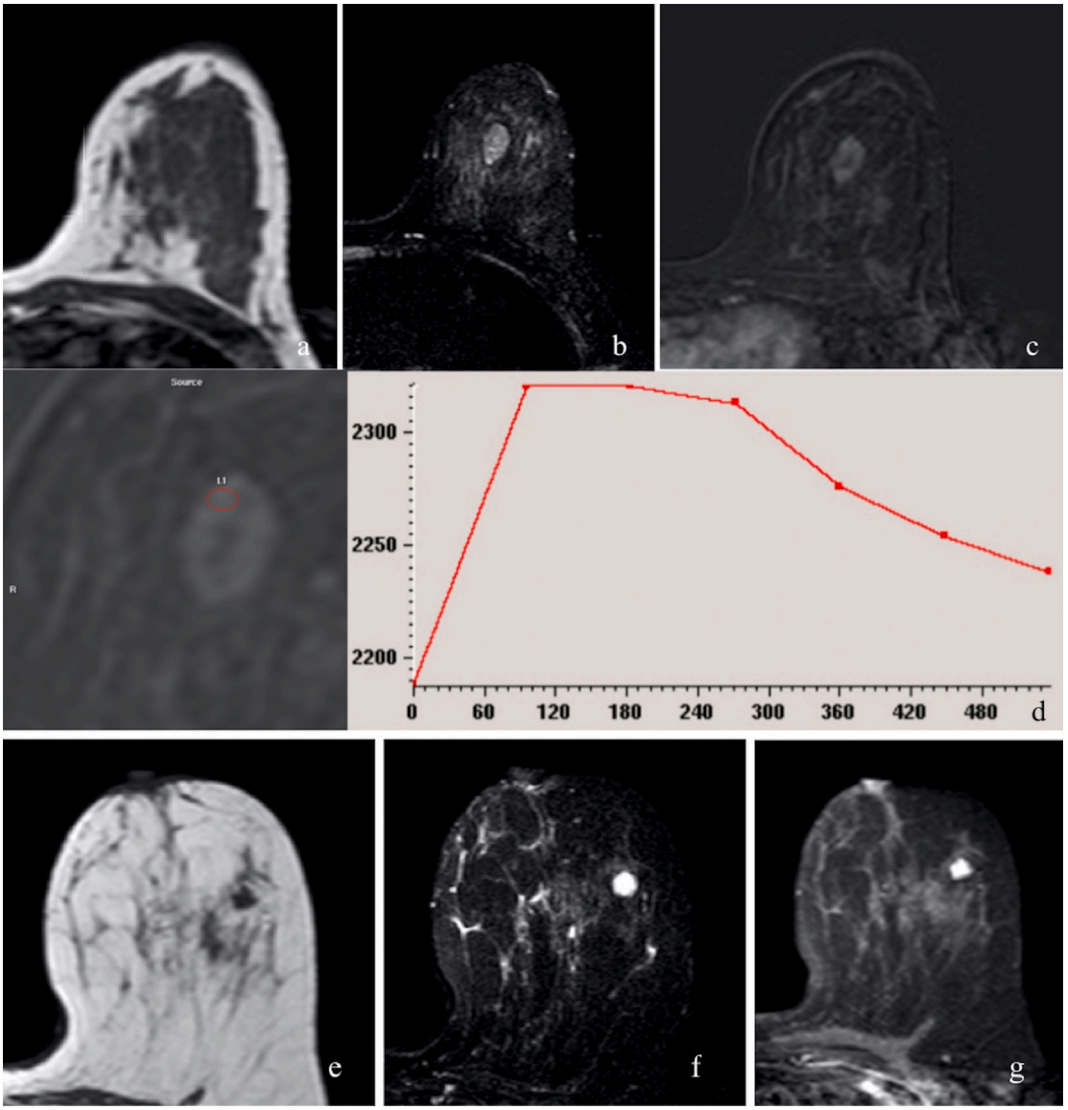


Fig. 14. MRI images, in 33-year-old female patient (a, b, c and d) and 48-year old female patient (e, f, g) with MFAs; the lesions are both hypointentense on T1 weighted images (a, e), isohyperintense (b) and hyperintense (f) on T2 weighted images. In dynamic sequences, the lesions show very low enhancement (d, g) with type 3 signal-intensity curve (d).

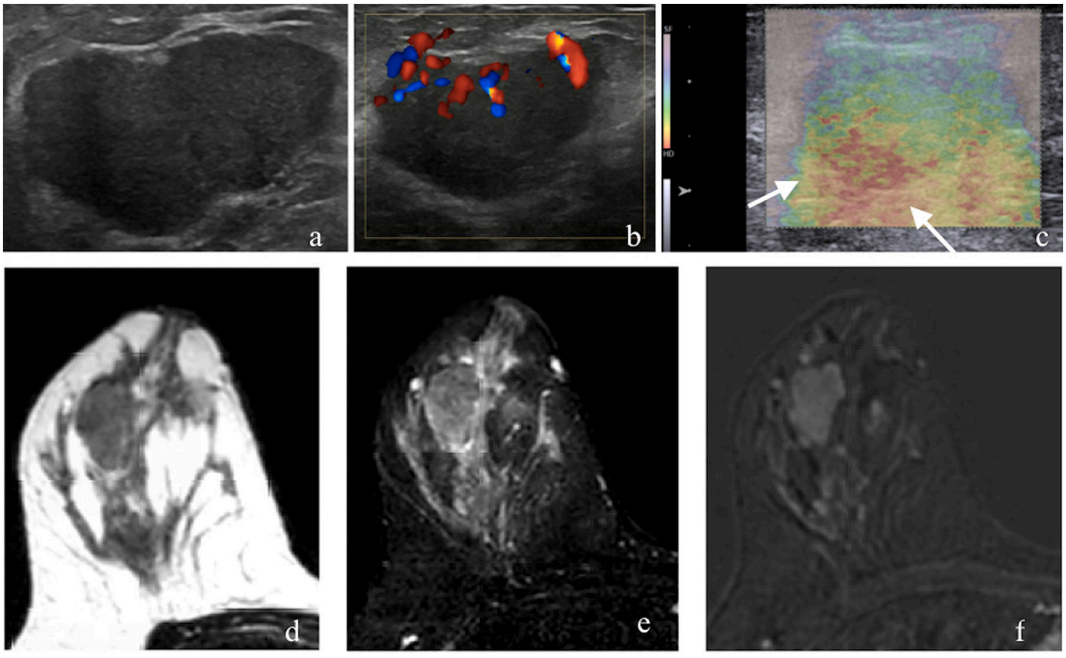


Fig. 15. B mod US (a), Doppler US (b), strain elastography (c) and MRI (d, e and f) images of a 27-year-old female patient with CeFA. The lesion is hypoechoic, oval shaped and well defined. In Doppler US image, there is mild vascularization and elastography shows focal stiffer area at the posterior part of the lesion (arrow). In MRI images, lesion is hypointense in both T1 (d) and T2 (e) weighted images. Dynamic sequence reveals diffuse enhancement (f). As a result of these imaging findings, core biopsy was applied, and the diagnosis was phyllodes tumour. After lesion excision, the diagnosis changed to CeFA.

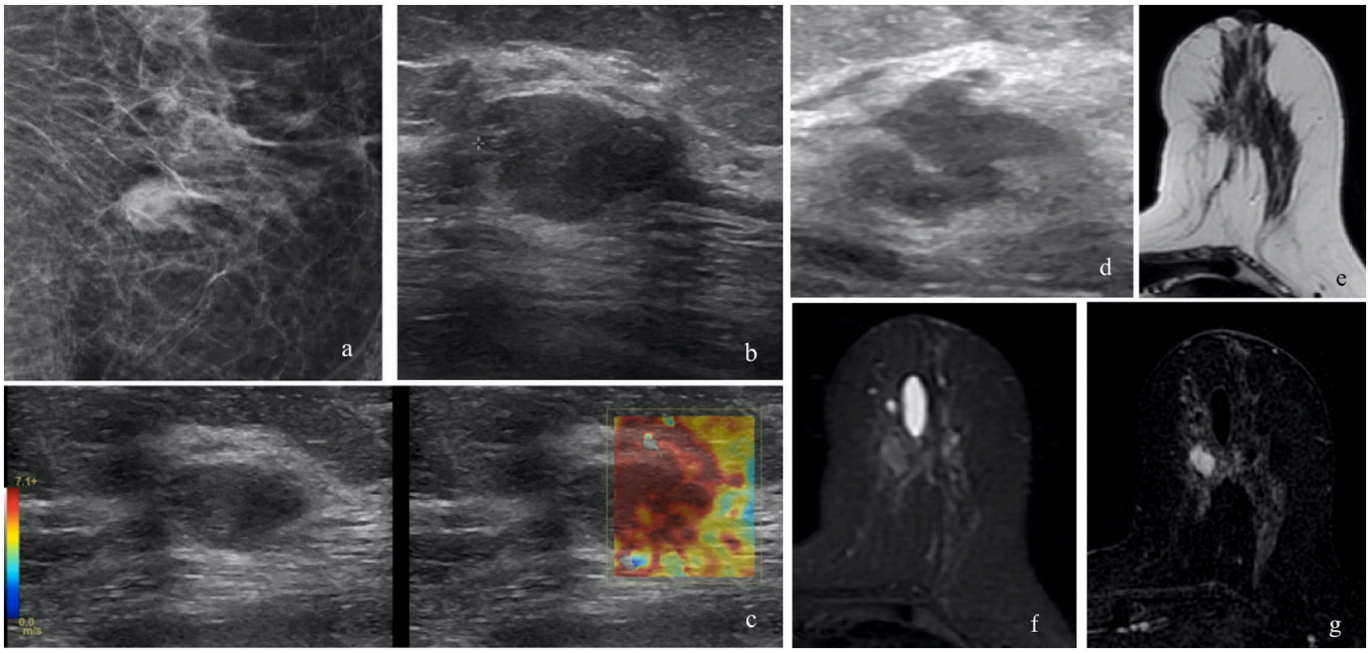


Fig. 16. Images of 42-year-old (a, b and c) and 35-year-old (d-f) female patients. MG image of the first patient shows round, hyperdense nodular lesion. Anterior contours of the lesion are obscured (a). US image revealed, well defines, solid, hypoechoic lesion. Lesion has semi-vertical orientation and posterior acoustic enhancement (b). The lesion has diffuse high stiffness in strain elastography (c). In B mod US image of the second patient, the lesion is in irregular shape and has non-circumscribed contours (d). MRI images show that, the lesion is hypointense on T1 weighted (e), iso-hypointense on T2 weighted (f) images and there is diffuse, prominent enhancement in dynamic sequence (g).

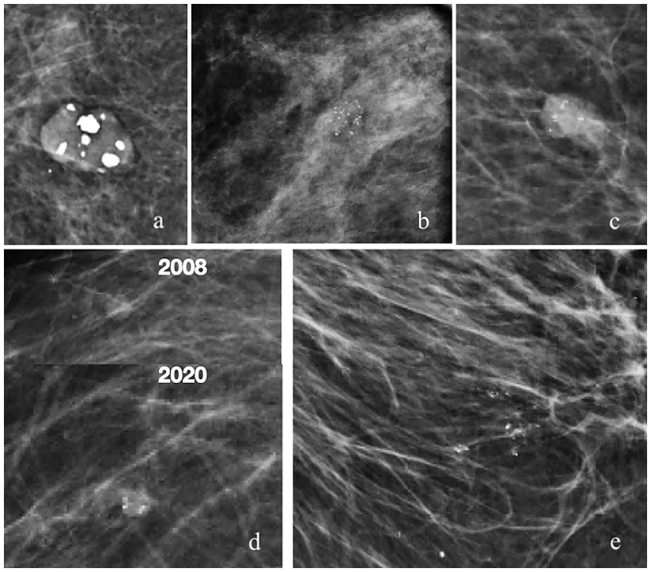


Fig. 17. MG images of different patients with HFA; there are benign, coarse calcifications (a). In another patient, there are clustered, pleomorphic calcifications (b). There are clustered, heterogeneous calcifications accompanied to nodular density (c). MG image realised in 2008 shows that, there is well defined, round nodular lesion. The MG image of the same patient in 2020 reveals that there are milimetric calcifications located at the marginal peripheral site of the lesion (d). Pleomorphic, branching, suspicious calcifications are seen in the last patient (e).

RADS 4 [48]. Notably, high enhancement and type 3 pharmacokinetic curves in MFAs, suspicious pleomorphic, branching calcifications in HFAs, and large dimensions in GFAs and JFAs are specific suspicious imaging findings leading to BI-RADS 4 classification [23,27,40,45].

Changes in the morphologic characterisations of the lesion, development of new calcifications, and an increase in size of >20% all can result in an upgrade from BI-RADS 3 to BI-RADS 4 [49]. Sonoelastographic findings, together with morphologic US characteristics, can lead to a classification change from BI-RADS 3 to BI-RADS 2 or 4 and further prospective studies with large series are needed to use these findings in daily practice [50,51].

Although there are different variants with different clinical characteristics, there are no consistent imaging finding for each type. For some variants, as they have different clinical findings and outcomes, the follow-up and treatment options have specific features. Although GFAs and JFAs are benign, they show rapid growth, which can cause aesthetic and clinical problems as a result of breast hypertrophy and asymmetry. Consequently, these lesions are typically treated by surgery [23]. Total surgical excision may be applied to CFAs and CeFAs diagnosed after core-needle biopsy [33,41]. As CFAs have a risk of developing malignancy, surgery provides a total cure [33,41]. Because CeFAs have overlapping features with those of PTs, surgery provides an exact diagnosis [33,41]. Both CeFAs which is a variant of fibroadenomas and PTs are fibroepithelial lesions. Fibroepithelial lesions are biphasic lesions showing epithelial and stromal proliferations. They include both benign and malignant forms. Benign fibroepithelial lesions include fibroadenoma, lactational adenoma and tubular adenoma whereas malignant ones include borderline/malignant PTs [1,52]. Close and careful radiologic follow-up is applied to both types of lesions after excision.

4. Conclusion

Fibroadenoma is the most common benign tumour of the breast. It is important to monitor for these lesions during daily, routine breast examinations. Knowledge about the existence of different fibroadenoma variants and their possible specific imaging findings contributes significantly to the evaluation and diagnosis of these lesions. Optimal diagnoses might provide us optimal patient evaluation, proper patient selection for surgeries or other interventions to lead the patient correct pathologic diagnosis.

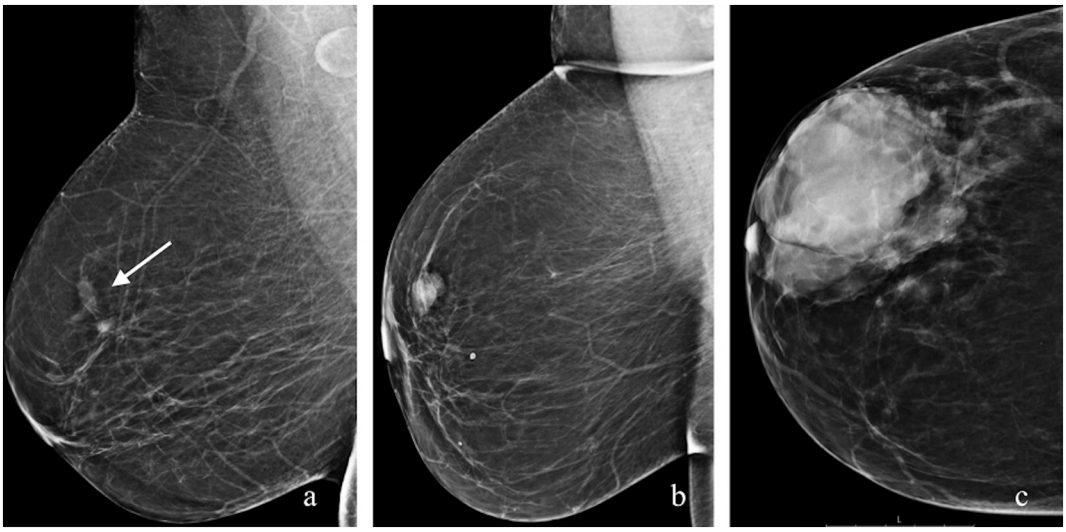


Fig. 18. MG images of HFA patients without calcifications; lesions can be hyperdense with indistinct (arrow) (a), circumscribed (b) and lobulated (c) margins.

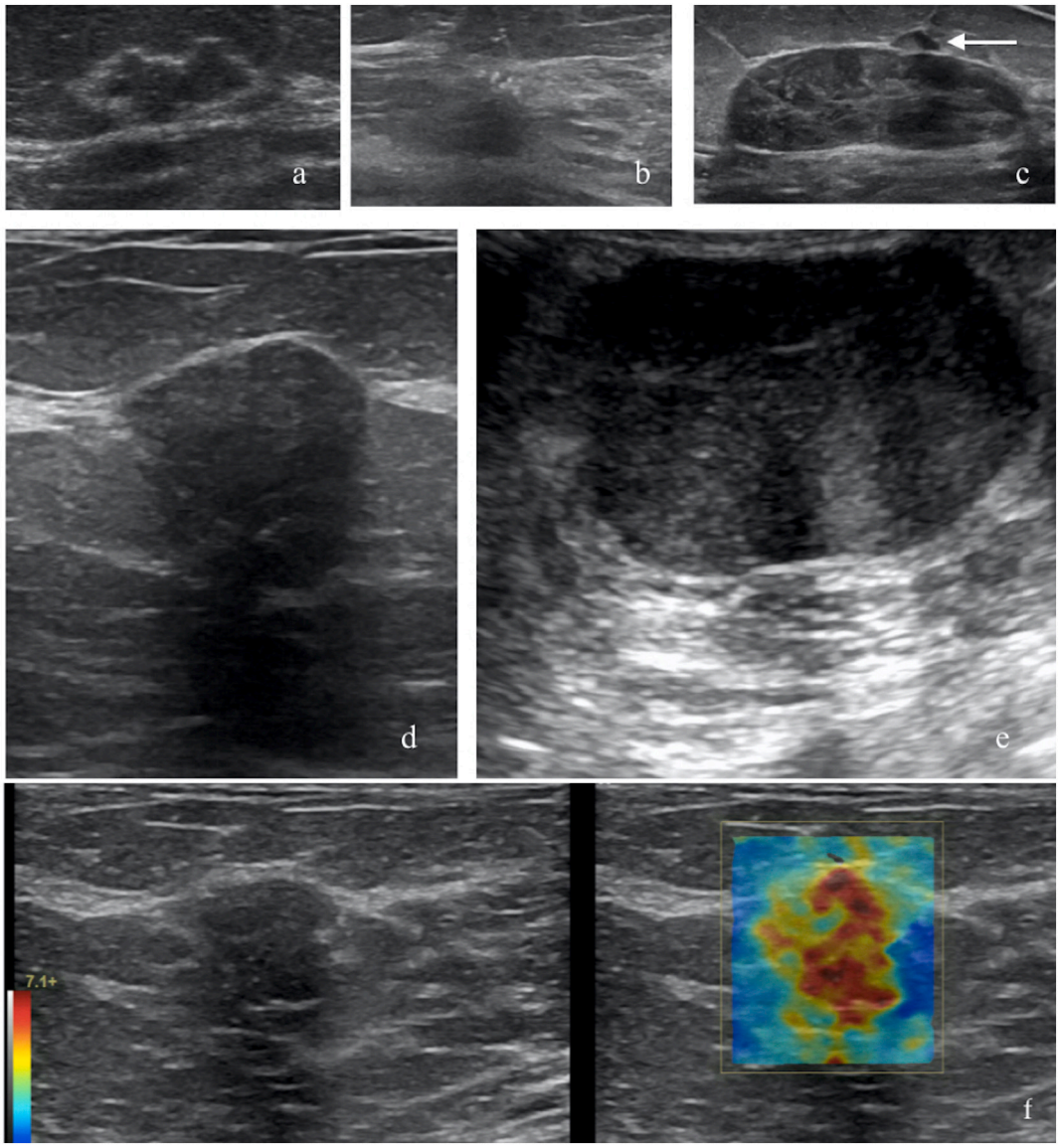


Fig. 19. B mod US images of different HFAs; the lesion is in irregular shapes and hypoechoic. There are increased perilesional echogenities compatible with the calcifications (a). In the second lesion, there is a heterogeneous and hypoechoic area including multiple milimetric calcifications (b). The third lesion has oval shape and there is a focal nodulation (arrow). The lesion is heterogeneous and has internal echogenities (c). There are oval, hypoechoic solid lesions with posterior acoustic shadowing (d) and enhancement (e). Strain elastography image shows high stiffness due to degeneration and hyalinization (f).

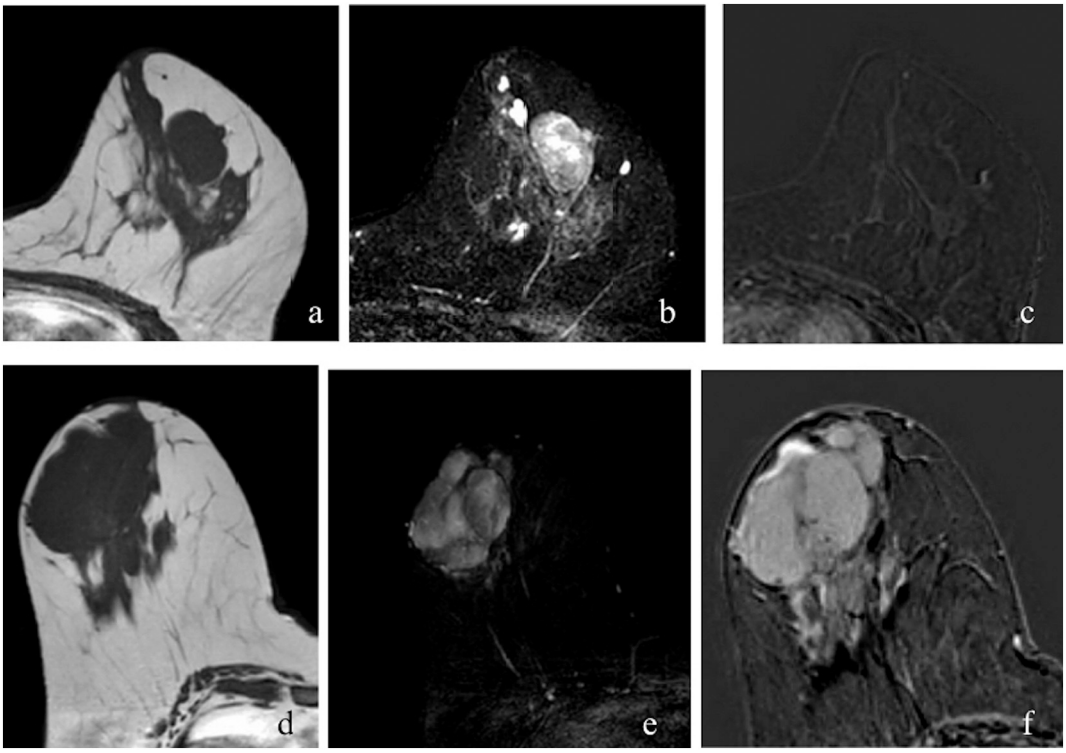


Fig. 20. MRI images, in 57-year-old female patient (a, b and c) and 42-year old female patient (d, e and f) with MFAs; the lesions are both hypointentense on T1 weighted images (a, d), hyperintense on T2 weighted images (b, e). In dynamic sequences, the lesion of the first patient do not show enhancement (c). However, in the second lesion, there is prominent enhancement (f).

References

[1] Chu B, Crystal P. Imaging of fibroepithelial lesions: a pictorial essay. Can Assoc Radiol J 2012;63:135–45. https://doi.org/10.1016/j.carj.2010.08.004.

[2] Goehring C, Morabia A. Epidemiology of benign breast disease, with special attention to histologic types. Epidemiol Rev 1997;19:310–27. https://doi.org/10.1093/oxfordjournals.epirev.a017960.

[3] Lee M, Soltanian HT. Breast fibroadenomas in adolescents: current perspectives. Adolesc Health Med Ther 2015;6:159–63. https://doi.org/10.2147/AHMT.S55833.

[4] Hughes LE, Mansel RE, Webster DJT. Aberrations of normal development and involution (ANDI): a new perspective on pathogenesis and nomenclature of benign breast disorders. Lancet 1987;2:1316–9. 1, https://doi.org/10.1016/s0140-6736(87)91204-9.

[5] Tavassoli FA. Biphasic tumors. In: Tavassoli FA, editor. Pathology of the breast. 2nd ed. Stamford, CT: Appleton & Lange; 1999. p. 571–631.

[6] Kleer CG, Tseng MD, Gutsch DE, et al. Detection of Epstein-Barr virus in rapidly growing fibroadenomas of the breast in immunosuppressed hosts. Mod Pathol 2002;15:759–64. https://doi.org/10.1038/modpathol.3880602.

[7] Krings G, Bean GR, Chen YY. Fibroepithelial lesions; the WHO spectrum. Semin Diagn Pathol 2017;34:438–52. https://doi.org/10.1053/j.semdp.2017.05.006.

[8] Soltanian H, Lee M. Breast fibroadenomas in adolescents: current perspectives. Adolesc Health Med Ther 2015;6:159–63. https://doi.org/10.2147/AHMT.S55833.

[9] Cole-Beuglet C, Soriano RZ, Kurtz AB, et al. Fibroadenoma of the breast: sonomammography correlated with pathology in 122 patients. AJR Am J Roentgenol 1983;140:369–75. https://doi.org/10.2214/ajr.140.2.369.

[10] Mitchell R, Kumar V, Nelson F, et al. Pocket companion to Robbins & Cotrans pathologic basis of disease. 8th ed. Elsevier Saunders; 2011. p. 550.

[11] Hanby A. Fibroepithelial neoplasms of the breast. Diagnostic Histopathol 2009;15:373–81. https://doi.org/10.1016/j.mpdhp.2009.05.002.

[12] Humphrey PA, Dehner LP, Pfeifer JD. The Washington manual of surgical pathology. 1st ed. Lippincott Williams & Wilkins; 2008. p. 262.

[13] Stavros AT. Benign solid nodules: specific pathologic diagnoses. In: Stavros AT, editor. Breast ultrasound. Philadelphia: Lippincott Williams & Wilkins; 2004. p. 528–96.

[14] Cole-Beuglet C, Soriano R, Kurtz AB, et al. Ultrasound, x-ray mammography and histopathology of cystosarcoma phylloides. Radiology 1983;146:481–6. https://doi.org/10.1148/radiology.146.2.6294737.

[15] Gokalp G, Topal U, Kizilkaya E. Power Doppler sonography: anything to add to BI-RADS US in solid breast masses? Eur J Radiol 2009;70:77–85. https://doi.org/10.1016/j.ejrad.2007.12.007.

[16] Strano S, Gombos EC, Friedland O, et al. Color Doppler imaging of fibroadenomas of the breast with histopathologic correlation. J Clin Ultrasound 2004;32:317–22. https://doi.org/10.1002/jcu.20041.

[17] Giuseppetti GM, Martegani A, Di Cioccio B, et al. Elastosonography in the diagnosis of the nodular breast lesions: preliminary report. Radiol Med 2005;110:69–76. https://doi.org/10.1002/jcu.20041.

[18] WHO position paper on mammography screening. World Health Organization; 2004.

[19] Elseedawy M, Whelehan P, Vinnicombe S, et al. Factors influencing the stiffness of fibroadenomas at shear wave elastography. Clin Radiol 2016;71:92–5. https://doi.org/10.1016/j.crad.2015.10.029.

[20] Hochman MG, Orel SG, Powell CM, et al. Fibroadenomas: variety of MR appearances with radiologic-histopathologic correlation. Radiology 1997;204:123–9. https://doi.org/10.1148/radiology.204.1.9205233.

[21] Davis S, Wallace A. A 19 year old with complete androgen insensitivity syndrome and juvenile fibroadenoma of the breast. Breast J 2001;7:430–3. https://doi.org/10.1046/j.1524-4741.2001.07610.x.

[22] Chung EM, Cube R, Hall GJ, et al. From the archives of the AFIP: breast masses in children and adolescents: radiologic-pathologic correlation. Radiographics 2009;29:907–31. https://doi.org/10.1148/rg.293095010.

[23] Cerrato F, Labow BI. Diagnosis and management of fibroadenomas in the adolescent breast. Semin Plast Surg 2013;27:23–5. https://doi.org/10.1055/s-0033-1343992.

[24] AbdelHadi M. Giant juvenile fibroadenoma: experience from a university hospital. J Family Community Med 2005;12:91–5. https://doi.org/10.1055/s-0033-1343992.

[25] Mendelson EB, Bohm-Velez M, Berg WA, et al. ACR BI-RADS atlas, breast imaging reporting and data system. Reston (VA): American College of Radiology; 2013.

[26] Kim SJ, Park YM, Jung SJ, et al. Sonographic appearances of juvenile fibroadenoma of the breast. J Ultrasound Med 2014;33:1879–84. https://doi.org/10.7863/ultra.33.11.1879.

[27] Baxi M, Agarwal A, Mishra A, et al. Multiple bilateral giant juvenile fibroadenomas of breast. Eur J Surg 2000;166:828–30. https://doi.org/10.1080/110241500447515.

[28] Arowolo OA, Akinkuolie AA, Adisa AO, et al. Giant fibroadenoma presenting like fungating breast cancer in a Nigerian teenager. Afr Health Sci 2013;13:162–5. https://doi.org/10.4314/ahs.v13i1.23.

[29] Hanna RM, Ashebu SD. Giant fibroadenoma of the breast in an Arab population. Australas Radiol 2002;46:252–6. https://doi.org/10.1046/j.1440-1673.2002.01054.x.

[30] Sharma S, Rana BP. Giant fibroadenoma of breast: a diagnostic dilemma in a middle aged woman. Adv Cytol Pathol 2017;2:109–12. https://doi.org/10.15406/acp.2017.02.00029.

[31] Kuiper A, Mommers EM, Wall E, et al. Histopathology of fibroadenoma of the breast. Am J Clin Pathol 2001;115:736–42. https://doi.org/10.1309/F523-FMJV-W886-3J38.
[32] Dupont WD, Page DL, Parl FF, et al. Long-term risk of breast cancer in women with fibroadenoma. N Engl J Med 1994;331:10–5. https://doi.org/10.1056/NEJM199407073310103.
[33] Greenberg R, Skornick Y, Kaplan O. Management of breast fibroadenomas. J Gen Intern Med 1998;3:640–5. https://doi.org/10.1046/j.1525-1497.1998.cr188.x.
[34] Sklair-Levy M, Sella T, Alweiss T, et al. Incidence and management of complex fibroadenomas. AJR Am J Roentgenol 2008;190:214–8. https://doi.org/10.2214/AJR.07.2330.
[35] Rosen PP. Rosen's breast pathology. 2nd ed. Philadelphia, PA: Lippincott Williams & Wilkins; 2001. p. 163–76.
[36] Pinto J, Aguiar AT, Duarte H, et al. Simple and complex fibroadenomas are there any distinguishing sonographic features? J Ultrasound Med 2014;33:415–9. https://doi.org/10.7863/ultra.33.3.415.
[37] Lozada JR, Burke KA, Maguire A, et al. Myxoid fibroadenomas differ from conventional fibroadenomas: a hypothesis-generating study. Histopathology 2017;71:626–34. https://doi.org/10.1111/his.13258.
[38] Koerner FC. Myxoid fibroadenoma. In diagnostic problems in breast pathology. Philadelphia: W.B. Saunders; 2009. p. 321–7.
[39] Courcoutsakis NA, Tatsi C, Patronas NJ, et al. The complex of myxomas, spotty skin pigmentation and endocrine overactivity (carney complex): imaging findings with clinical and pathological correlation. Insights Imaging 2013;4:119–33. https://doi.org/10.1007/s13244-012-0208-6.
[40] Klinger K, Bhimani C, Shames J, et al. Fibroadenoma: from imaging evaluation to treatment. J Am Osteopath Coll Radiol 2019;8:17–30.
[41] Edwards T, Jaffer S, Szabo JR, et al. Cellular fibroadenoma on core needle biopsy: management recommendations for the radiologist. Clin Imaging 2016;40:587–90. https://doi.org/10.1016/j.clinimag.2016.02.009.
[42] Lawton TJ, Acs G, Argani P, et al. Interobserver variability by pathologists in the distinction between cellular fibroadenomas and phyllodes tumors. Int J Surg Pathol 2014;22:695–8. https://doi.org/10.1177/1066896914548763.
[43] Foster ME, Garrahan N, Williams S. Fibroadenoma of the breast: a clinical and pathological study. J R Coll Surg Edinb 1988;33:16–9.
[44] Sewell CW. Pathology of benign and malignant breast disorders. Radiol Clin North Am 1995;33:1067–84. https://doi.org/10.1177/1066896914548763.
[45] Lanyi M. Diagnosis and differential diagnosis of breast calcifications. New York, NY: Springer-Verlag; 1988. p. 145–56.
[46] Morris EA. Breast magnetic resonance imaging lexicon. In: Morris EA, Liberman L, editors. Breast MRI. New York- NY: Springer; 2005. p. 51–78.
[47] Stavros AT, Thickman D, Rapp CL, Dennis MA, Parker SH, Sisney GA. Solid breast nodules: use of sonography to distinguish between benign and malignant lesions. Radiology 1995;196:123–34. https://doi.org/10.1148/radiology.196.1.7784555.
[48] Gordon PB, Gagnon FA, Lanzkowsky L. Solid breast masses diagnosed as fibroadenoma at fine-needle aspiration biopsy: acceptable rates of growth at long-term follow-up. Radiology 2003;229:233–8. https://doi.org/10.1148/radiol.2291010282.
[49] Cho N, Lim J, Moon WK. Usefulness of ultrasound elastography in reducing the number of breast imaging reporting and data system category 3 lesions on ultrasonography. Ultrasonography 2014;33:98–104. https://doi.org/10.14366/usg.13024.
[50] Chopier J, Dratwa C, Antoine M, et al. Radiopathological correlations: masses, non-masslike enhancements and MRI-guided biopsy. Diagn Interv Imaging 2014;95:213–25. https://doi.org/10.1016/j.diii.2013.12.007.
[51] Klotz T, Boussion V, Kwiatkowski F, et al. Shear wave elastography contribution in ultrasound diagnosis management of breast lesions. Diagn Interv Imaging 2014;95:813–24. https://doi.org/10.1016/j.diii.2014.04.015.
[52] Wiratkapun C, Piyapan P, Lertsithichai P, et al. Fibroadenoma versus phyllodes tumor: distinguishing factors in patients diagnosed with fibroepithelial lesions after a core needle biopsy. Diagn Intervent Radiol 2014;20:27–33. https://doi.org/10.5152/dir.2013.13133.